International Journal of Pure and Applied Mathematics
Volume 86 No. 4 2013, 653-667
ISSN: 1311-8080 (printed version); ISSN: 1314-3395 (on-line version)
url: http://www.ijpam.eu
doi: http://dx.doi.org/10.12732/ijpam.v86i4.6

DESIGN OF 100 kHz SONAR FOR MARINE MAPPING APPLICATIONS

R. Sathishkumar[1 §], T.V.S. Prasad Gupta[2], M. Ajay Babu[3], Habibullakhan[4]
Department of Electronics and Communication Engineering
KL Universit
Green Fields, Vaddeswaram, Guntur District, A.P., 522 502, INDIA

Abstract: Side scan sonar (SSS) is an important mapping tool in underwear imaging system. This paper provides sufficient information on SSS design. SSS is known for very high quality, high resolution, ocean bottom imaging. It is able to rapidly survey large ocean areas for bottom and suspended sea-mines or other kinds of threats. Another operational aspect of these systems is that they allow autonomous underwater vehicles (AUVs) to conduct operations, mostly in shallow water and near land. It produces a representation in image form of the seabed; however, no closed form analytic expression or direct modeling technique exists to represent this complex process. In this paper the basic principle is presented for a model for the simulation of SSS, which produces as its output a qualitative image of the form generated by the actual SSS. The model considers the underlying physical processes including the effects of the refractive water medium, the scattering from the seabed and the transducer motion and directivity characteristics. Further, this work concerns the design and analysis of SSS via MATLAB simulation in order to satisfy the operational requirements. Moreover, this research has tried to indicate the various problems that may arise when a SSS operates in its near-field region and suggests certain solutions. The active sonar equation and its factors were explained and were evaluated.

AMS Subject Classification: 37N10, 86A05
Key Words: sonar, mapping, analytic signal

Received: March 7, 2013

§Correspondence author

1. Introduction

Side scan sonar (SSS) is well known for high quality, high resolution, ocean bottom imaging. This work concerns on design and simulation SSS, which is used for bathymetric surveys, commonly called seafloor mapping, by almost all navies throughout the world and also for other naval operations (see [1]-[4]). We made an attempt to establish a logical and systematic set of procedures that will help in design and analyze the performance of a SSS in order to satisfy different operational requirements. In this work sufficient information on SSS parameters are provided, to make it easy for any researcher to select the right design for the corresponding application. Based on its high accuracy in ocean bottom imaging, a SSS can rapidly survey large ocean areas for bottom and suspended sea mines or other kind of threats. It can also be used for search and rescue operations in deep or shallow waters. SSS is currently used on Autonomous Underwater Vehicles (AUVs) in order to provide information about the seafloor (especially in shallow water) and help AUVs navigate underwater or locate mines and other objects of interest on the bottom of the sea (see [5]).

2. Side Scan Sonar Operation

The SSS consists of a transducer moving in a straight line and transmits a signal and records the echoes that are stacked sequentially to construct a raster scan image of the sea floor as shown in Figure 1. Angles are estimated for each received echo through beamforming algorithms, and angle together with distance (time) gives us the polar coordinates.

The range resolution is the distance between the -3dB points of the main lobe of the transmitted signal as measured along the range axis. The range resolution is proportional to the inverse of the bandwidth of the transmitted signal, see [6]. The area coverage rate indicates the amount of area per unit time is the product of the range and swath width. The frequency of the SSS gives a maximum range capability, acoustic wavelength and the lower limit on the size of objects. To reduce the sensitivity of the height accuracy losses, multiple estimates of the height can be formed from independent looks of the scene, see [7]. It builds up a 2-D picture of the sea bed using a combination of an asymmetrical transducer and the motion of the sonar platform through the water, see [8]. The transducer may be mounted on the keel of a ship or be located in a towed body. A towed body will have the advantage of depth capability. As the ship moves, therefore, successive pings build up the map of the sea bed. If

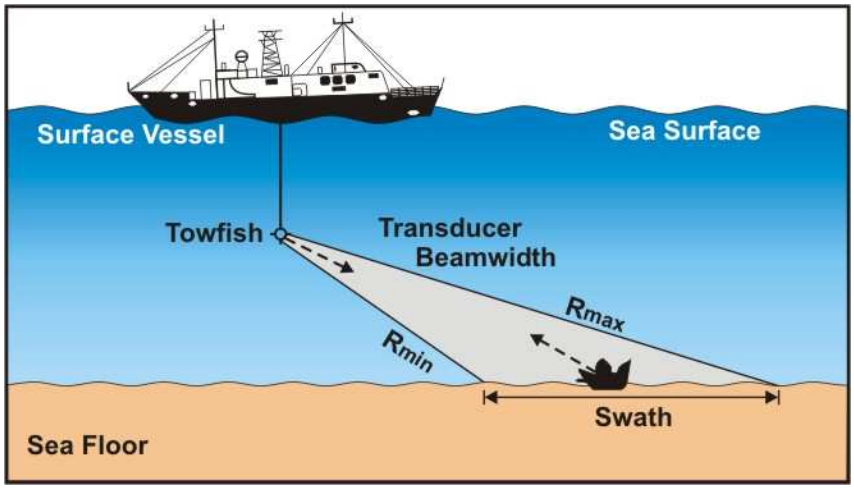

Figure 1: Overview Side Looking Sonar

the bottom is smooth, the display will simply show a characterless, noise-like picture. If, however, the sea bed has features, such as peaks and valleys, the picture will be quite different; the peaks will backscatter strongly and the valleys, shielded by the peaks, will display as shadows. Objects on the sea bed - wrecks, mines and bottomed submarines - are frequently detected by their shadows. This mechanism is very important for the detection and classification of bottom mines. Because of their very low target strengths, echoes from mines are very difficult to detect against a background of bottom reverberation; the shadowgraph can, however, indicate the presence of a mine even when its echo is hidden by the reverberation, see [9]-[10].

3. Design of the System

In order to proceed with the analysis of a SSS design, we define the concepts and parameters with which we will deal the analysis. In this work, a SSS is modeled as shown in Figure 2. The form of the transmitted pulse has an arbitrary function p(t) then the received pulse is

$$r\,(t) = p(t - \frac{2r}{c}), \tag{1}$$

where r is the range to the reflecting object and c is the speed of sound in the medium. The propagation of sound through medium properties can be

described by

$$\frac{\partial^2 \emptyset}{\partial t^2} = c^2 \nabla^2 \emptyset. \tag{2}$$

The analytic form of a function $f(x)$ is formed by adding $jf(x_1)$ to the original function, where $jf(x_1)$ is the conjugate function of $f(x)$ derived using the Hilbert Transform. The analytic function will be denoted using the subscript +

$$f_+(x) = f(x) + jf(x_1). \tag{3}$$

For example, if $f(x) = A\sin(x)$, the conjugate function $f(x_1) = A\cos(x)$ hence the analytic form of $A\sin(x)$ is

$$A\sin_+(x) = A\sin(x) + jA\cos(x). \tag{4}$$

Expanding the $\sin(x)$ and $A\cos(x)$ function to their complex forms

$$f_+(x) = \frac{A}{2}\left(e^{jx} + e^{-jx}\right) + j\frac{A}{2j}(\left(e^{jx} + e^{-jx}\right) = Ae^{jx}. \tag{5}$$

The analytic function has the property that the Fourier transform if $f_+(x)$ has only positive frequency components. The Baseband signal is obtained by multiplying the analytic signal by the normalized complex conjugate of the centre frequency

$$A\sin_{+bb}(x) = A\sin_+(x).e^{-jx} \quad = A \tag{6}$$

For real data, the analytical signal can be formed by eliminating the negative frequencies from the spectrum of the real signal and doubling the resulting spectrum. Hence

$$X_+(f) = \begin{cases} 2X(f) & \text{if } f > 0, \\ X(f) & \text{if } f = 0, \\ 0 & \text{if } f < 0. \end{cases} \tag{7}$$

The baseband signal can be obtained by multiplication by the complex vector representing the conjugate of the centre frequency. The time between transmitting consecutive pulses, the pulse repetition frequency (PRF), must be large enough to ensure that the echo returns from the previous pulse do not interfere with those from the current pulse. For a short pulse, the minimum pulse repetition interval PRF for unambiguous imaging of targets up to a distance r is

$$PRF = \frac{2r}{c} \tag{8}$$

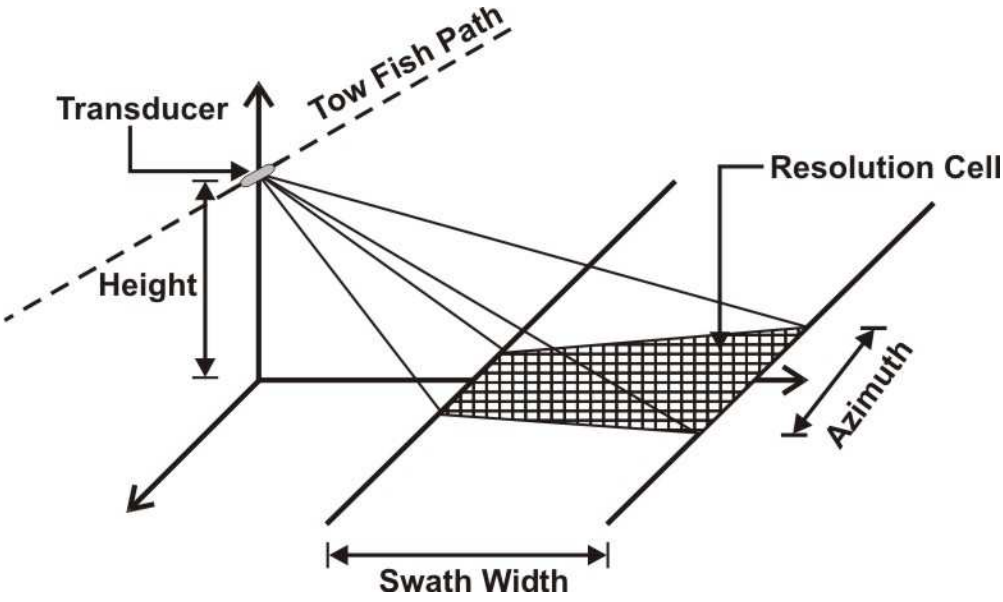

Figure 2: Imaging geometry of SSS

In practice the PRF must be much larger than this to ensure returns from targets beyond the nominal imaging range are sufficiently attenuated so as not to interfere with the image. In the sonar system, if the emitted pulse has duration of τ_p the range resolution of the system will be $c\tau_p/2$, i.e. half the pulse length. Hence the resolution is inversely proportional to the pulse length, suggesting a very short pulse length should be used to obtain maximum range resolution. In the limiting case (for maximum resolution), the pulse tends to an impulse, hence, the required bandwidth of the transmitter / receiver tends to infinity. More importantly, the required transmitter power for a given signal to noise ratio also tends to infinity. Some of the problems associated with transmitting and receiving an impulse can be overcome by the use of a long modulated pulse and the use of pulse compression processing in the receiver. The most popular pulse function is the linear FM (LFM) chirp. The range resolution of a system using an FM chirp can be shown to be related only to the bandwidth of the emitted chirp, and unrelated to the duration of the chirp. Hence a long duration pulse can be used, and the problems of finite transmitter power outlined above can be greatly reduced. A chirp $p_{(t)}$ of duration τ_p and centre frequency f_c is

$$p(t) = rect\,(t/\tau_p)\cos[2\pi\left(f_c t + Kt^2/2\right)],$$

where time t is bounded by $\frac{\tau_p}{2}<t<\frac{\tau_p}{2}, and K is the chirp rate.$ For an 'up' chirp K = B/τ_p and for a 'down' chirp K= - B/τ_p where B is the bandwidth of the chirp. The analytic form of the chirp function is

$$p_+(t) = rect(t/\tau_p)e^{j\frac{2\pi Kt^2}{2}}e^{j2\pi f_c t} \tag{9}$$

The baseband form of $p_{+(t)}$ can be obtained by multiplying $p_+(t)$by the analytic form of a function for the centre frequency, in this case $\cos_+(2\pi f_c t) = e^{-j2\pi f_c t}$. Hence the complex baseband form of the chirp is

$$p_{+bb}(t) = rect(t/\tau_p)e^{j2\pi Kt^2/2} \tag{10}$$

The function for the transmitted chirp in the frequency domain is

$$p_{tx+bb}(f) = \sqrt{j/K\pi} \quad rect\,(f/K\tau_p)\exp(-j\pi f^2/K) \tag{11}$$

If reflections are received from a target, the received signal will be the transmitted pulse delayed by $d = 2r/c$,equal to the time the pulse has been in the water. The Fourier transform of the received chirp can be written

$$p_{rx+bb}\,(f) = \sqrt{j/K\pi}\exp\,(-j2\pi f_c d)\exp\,(-j2\pi f d)\,rect\,(f/K\tau_p)\exp\left(-j\pi f^2/K\right). \tag{12}$$

The matched filter is the complex conjugate of the transmitted pulse. The Fourier transform of the matched filter can be written

$$H_{+bb}(f) = 1/\sqrt{jK}rect(f/K\tau_p)\exp(j\pi f^2/K). \tag{13}$$

The pulse compressed received chirp, $G(f)$, is obtained by multiplying the received chirp with the transfer function of the matched filter.

$$G_f = p_{rx+bb}(f)\,.H_{+bb}(f),$$

$$G(f) = 1/K\pi\exp\,(-j2\pi f_c d)\exp\,(-j2\pi f d)\,rect(f/K\tau_p). \tag{14}$$

Taking the inverse Fourier transform

$$g(t) = \frac{K\tau_p}{\pi}\exp\,(-j2\pi f_c d)\sin[\pi K\tau_p\,(t-d)\,]. \tag{15}$$

Recalling $B = K\tau_p, d = 2r/c and = c/f_c$

$$g(t) = B/\pi\exp\,(-j4\pi r/\lambda)\,sinc[\pi B\,(t-2d/c)\,] \tag{16}$$

Hence pulse compression of a chirp function using a matched filter compresses the received chirp into a sinc function of the bandwidth. The peak is at 2d/c. The first nulls of the function are at 1/B, and the half power points lie at approximately 1/2B.The 3dB range resolution can therefore be considered to be approximately c/2B. The range resolution of a sonar system using a LFM pulse is dependent on the bandwidth of the transmitted pulse. If no window function is used on the matched filter, the -3dB range resolution is c/2B. The shape of the pulse compressed function can be changed by use of a window, or weighting, function applied to the matched filter. The effects on pulse width and side lobe level of a number of common window functions are shown in Figure 3. The raised cosine or Hamming window is the most commonly used window function

$$W_{Han}(t) = 0.5 + 0.5\cos(2\pi t/\tau_p) \tag{17}$$

Along with Hamming Window

$$W_{Ham}(t) = 0.54 + 0.46\cos(2\pi t/\tau_p) \tag{18}$$

For very high side lobe reduction, the Blackmans – Harris window can be used given by

$$W_{B-H}(t) = a_o + a_1\cos(2\pi t/\tau_p) + a_2\cos(2\pi 2t/\tau_p) + a_3\cos(2\pi 3t/\tau_p). \tag{19}$$

Here $a_o = 0.35875$, $a_1 = 0.48829$, $a_2 = 0.14128$ and $a_3 = 0.01168$. The pulse compressed functions using Hamming, and Blackman-Harris weighting are compared to the case with no weighting in Figure 3. It can be seen applying a window function has the effect of reducing the side lobe level at the expense of broadening the main peak. It is recommended that the Hanning or Hamming window is used because this gives a good compromise between shadow depth and image resolution. A situation where very high side lobe suppression is desirable is when the scene consists of one, or a number of very strong point scatterers against a 'dark' background. In such a situation, the Blackman-Harris window can be used to prevent the sidelobes from the strong scatterers spreading into the surrounding area. It is shown that the minimum range of a sonar system is dependent on both the length of the pulse used and the delay between transmitting and sampling. The pulse compressed signal is obtained by convolving the raw received data with the appropriate matched filter. For large data sets this process is most efficiently performed in the frequency domain.

As a standard practice, the raw data and the matched filter must be appropriately zero padded before the convolution to avoid aliasing caused by wrap around effects. Usually in FFT convolution the zero padding is removed from

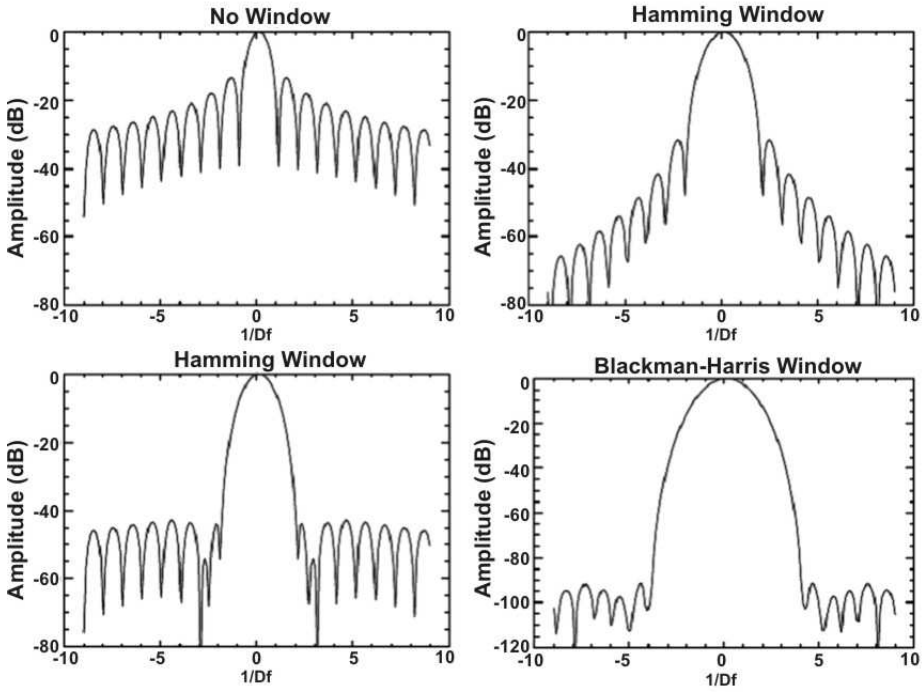

Figure 3: Windowing function

the resulting data, however in the case of sonar pulse compression this extra data represents an area of sea bed and therefore contains useful information. The process is shown in Figure 4. The sampling starts at a time d_{samp} after transmission of the ping, and continues for a time npts/$f_s$where npts is the number of samples and f_s is the sampling frequency. The central part of the range compressed data has the theoretical maximum range resolution because the whole matched filter is used. The outer edges of the data have a reduced resolution because only part of the matched filter, hence a lower bandwidth, is used in the convolution; the resolution becomes gradually worse towards the edge of the data. The minimum range of the system

$$r_{min} = (d_{samp} - \tau_p)\, c/2. \tag{20}$$

The factor of 2 in the denominator comes from the fact range is derived from the two way travel time.

$$r_{max} = (d_{samp} + npts/f_s)\, c/2. \tag{21}$$

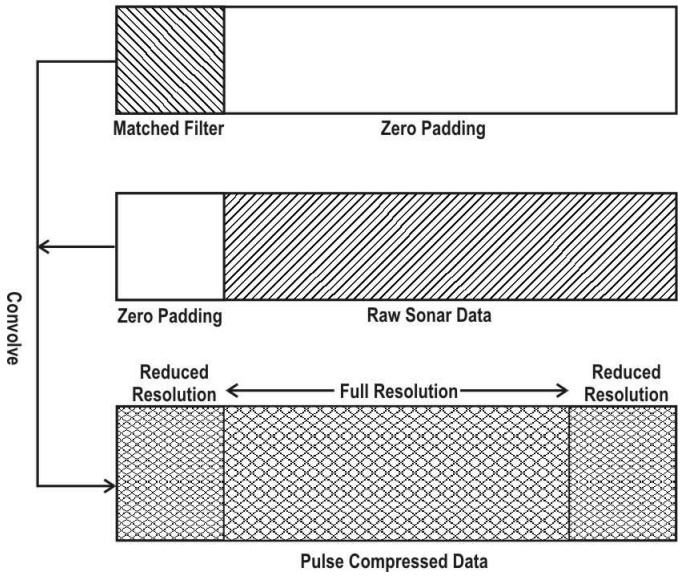

Figure 4: Convolution processes

4. Phase Centre Approximation

A transmitter TX is separated a distance $\Delta s$from a receiver RX. The phase centre C is located half way between the transmitter and receiver as shown in Figure 5. The system is imaging a target at T located at an angle θ from boresight. The error in making the phase centre approximation is the difference in path length between the bistatic path length TXT+TRX and the monostatic path length 2CT. This error is given by

$$TXT + TRX - 2CT = \frac{\Delta s^2}{4r^2}\cos^2(\theta) + \frac{\Delta s^2}{16r^3}\cos^2(\theta)\left(1 - 5/4\cos^2(\theta)\right). \quad (22)$$

Taking the first term in the series, it can be seen that the phase centre approximation holds r$> > \Delta s^2/4\lambda$.. The phase centre approximation is also valid in the near field so long as the received signal is advanced by $\frac{\Delta^2}{4rc}$ and the transmission sector satisfies

$$\frac{\Delta s^2}{4r\lambda}(1 - \cos^2\theta_e) \ll 1,$$

where θ_e is the half transmission beamwith.

A sonar system consisting of just one transmitter and receiver can detect the range of a target, although the position of the target is ambiguous along

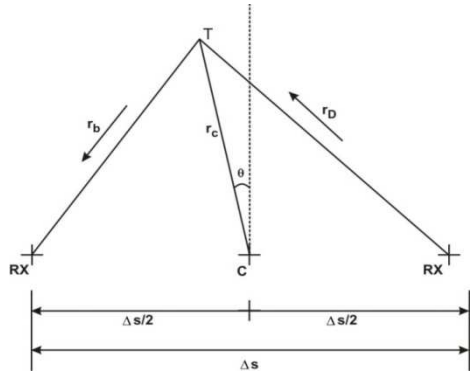

Figure 5: Phase centre approximation

an arc within the transmitter and receiver beam widths. Increased angular resolution can be obtained by summing the received signals along an array of receivers. This technique is commonly used in both sonar and radar. By applying suitable delays to the received signals, the direction of the receiver beam can be changed, a technique called beamsteering. A further increase in resolution can be obtained using focused beamforming where the received signal is focused to each point in the desired beam pattern. If a plane wave front arriving at any array of N hydrophones spaced at distance $\Delta ralong$the x axis. The wave front has a special spatial angular frequency (radius per unit distance) of |k|=2π /λ travelling in the direction k. At a given point s(x,y) the wavefront may be described as

$$p_+(s,t) = \exp\left[j\left(\omega t - k.s\right)\right], \tag{23}$$

where ω is the angular frequency of the wave.

The base banded form is

$$p_{+bb}(x,y,t) = \exp\left(-jk_x x\right)\exp\left(-jk_y y\right). \tag{24}$$

The receiver array is placed along the x axis, hence the component of K along the array is

$$k_x = |k|\, sin\theta = (2\pi/\lambda) sin\theta. \tag{25}$$

The wave front seen by the receiver array is therefore

$$p_{+bb}(x,t) = \exp\left(-jk_x x\right). \tag{26}$$

The wavefront can be sampled by the receivers $n = 0, 1, 2 \ldots N-1$, which are located at positions $x = \Delta r, 2\Delta r, \ldots (N-1)\Delta r$ along the x axis. The output

of the n-th sensor is therefore

$$p_{+bbn}(t) = \exp(-jk_x n\Delta r). \tag{27}$$

The summation of the outputs from all sensors is

$$p_{+bbn}(t) = \sum_{n=0}^{N-1} \exp[-jn\,(k_x\Delta r)\,]. \tag{28}$$

Re-arranging and substituting $k_x\Delta r = K$

$$p_{+bbn}(t) = 1 - \frac{\exp\,(-jNK)}{1-\exp(-jK)}, \tag{29}$$

$$p_{+bbn}(t) = [\frac{\exp(-jNK/2)}{\exp(-K/2)}][\frac{\exp\,(-jNK/2) - \exp(-jNK/2)}{\exp\,(jK/2) - \exp(-jK/2)}], \tag{30}$$

$$p_{+bbn}(t) = \exp\,[-jK/2\,(1-N)\,]\frac{\sin(NK/2)}{\sin(K/2)} \tag{31}$$

The form of the phase term is $\exp[-jk/2(1-N)$ and an amplitude term

$$\frac{\sin\,(NK/2)}{\sin\,(K/2)}$$

Substituting $K = k_x\Delta r$, and $k_x = 2\pi\sin\,(\theta)\,/\lambda$ into the amplitude term, gives an equation for the beam pattern in angle θ:

$$p_{+bb}(\theta) = \frac{\sin(N\pi/\lambda)\Delta r\sin(\theta)}{\sin(\pi/\lambda)\Delta r\sin(\theta)}. \tag{32}$$

5. Simulation Studies

Simulation is an important tool in the research and development of signal processing, a key part of a sonar system, that permits the study of sonar performance and robustness, also it gives the analyst the opportunity to investigate variations in the sonar results as a function of one system parameter, whilst keeping other parameters fixed, hereby enabling sensitivity studies. A sonar simulator can be used as well for image data base generation, as an addition to costly measured data of which there is typically a shortage. A data base with sufficient actuality and variability is crucial for testing and developing signal

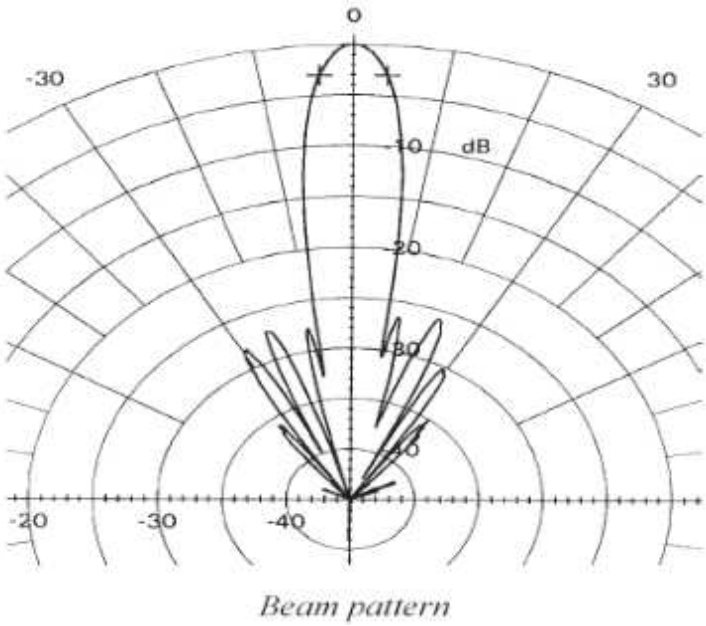

Figure 6: SSS beam pattern

processing algorithms for sonar image analysis, such as object detectors and classifiers. Parameters of the SSS for the present study is as follows

Maximum Range: 200m;

Frequency: 100 kHz;

Pulse Length: 133 μs;

Source Level: 204 dB.

The Figures 6, 7, and Figure 8 shows the Beam pattern, beam pattern vs steering angle and Simulation result.

6. Conclusion

In this, a near-field operation is considered when a SLS is operating in shallow water environments. This work was based on the assumptions that the platform of the SLS moves with a constant speed and maintains a constant altitude above the ocean bottom. It would be important to perform research in cases where the speed of the platform and the altitude are not constant. A separate important task would be to research various signal processing methods that may be used for beamforming for planar arrays for SSS applications. The signal processing

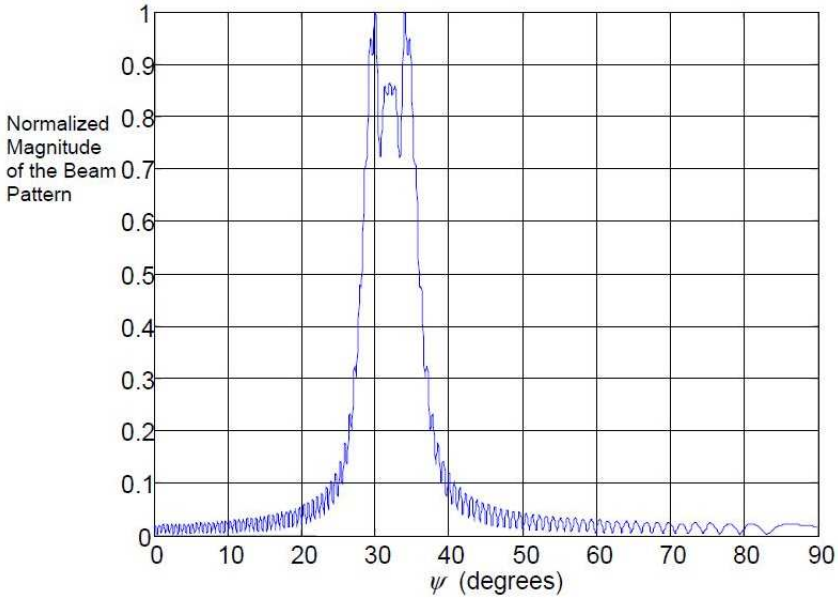

Figure 7: Beam pattern vs beam steering angle

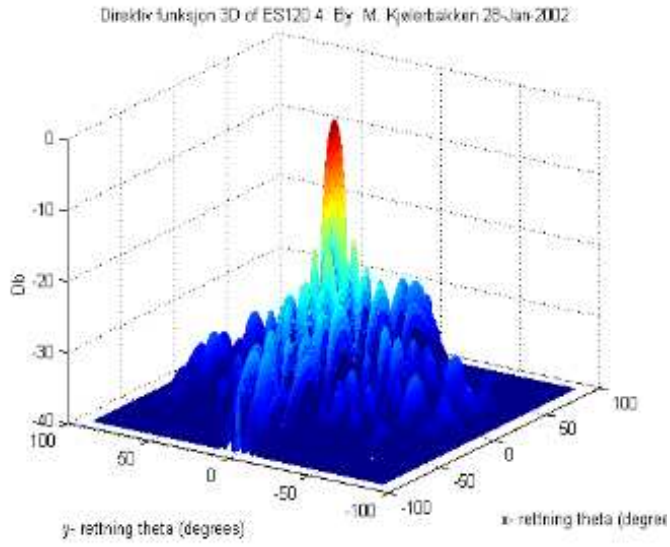

Figure 8: SSS simulation

algorithms would need to be examined from the performance point of view for various operational scenarios (far-field and near-field) with different operational goals.

Acknowledgments

We are grateful to the management of the KL University for providing the necessary facilities for the stimulating research environment. We received continual encouragement from Prof.Dr. Shree Hari Rao, Vice Chancellor of the KL University. We received a lot of guidance from Dr.Dhilsha Rajappan, Joint Project Director of National Institute of Ocean Technology–NIOT, India, who provided us the initial desire, interest and ideas on ocean engineering projects. We extend our thanks to Prof. N. Venkatram, Dean of Electrical Sciences of, KL University for his continual encouragement on the research work.

References

[1] F. Langner, C. Knauer, W. Jans, A. Ebert, Side scan sonar image resolution and automatic object detection, classification and identification, *OCEANS 2009 - EUROPE, 11-14 May 2009* (2009), 1-8.

[2] Zhao Jianhu, Tao Weiliang, Zhang Hongmei, Yang Kun, Study on side scan sonar image matching based on the integration of SURF and similarity calculation of typical areas, *OCEANS 2010 IEEE - Sydney, 24-27 May 2010* (2010), 1-4.

[3] J. Fawcett, V. Myers, D. Hopkin, A. Crawford, M. Couillard, B. Zerr, Multiaspect classification of sidescan sonar images: four different approaches to fusing single-aspect information, *IEEE Journal of Oceanic Engineering*, **35**, No. 4 (2010), 863-876.

[4] R.T. Quintal, J.E. Kiernan, J. Shannon, P.S. Dysart, Automatic contact detection in side-scan sonar data, *IEEE International Conference on Technologies for Homeland Security (HST)* (2010), 270-275.

[5] E. Chen, Huang Sheng-Wei; Wang Wei-Han; Gao Jen-Hwa, Side scan sonar grid map for unmanned underwater vehicle navigation, *OCEANS 2011* (2011), 1-8.

[6] M.F. Fallon; M. Kaess, H. Johannsson, J.J. Leonard, Efficient AUV navigation fusing acoustic ranging and side-scan sonar," Robotics and Automation (ICRA), *International Conference on 2011 IEEE* (2011), 2398-2405.

[7] Val E. Chmidt, Tom C. Weber, Arthur C. Trembanis, Automated optimal processing of phase differencing side-scan sonar data using the most-probable angle algorithm, *Oceans* (2012), 1-6.

[8] N. Kumar, Qun Feng Tan, S.S. Narayanan, Object classification in sidescan sonar images with sparse representation techniques, *2012 IEEE International Conference on Acoustics, Speech and Signal Processing (ICASSP)* (2012), 1333-1336.

[9] P. Vandrish, A. Vardy, D. Walker, O.A. Dobre, Side-scan sonar image registration for AUV navigation, *2011 IEEE Symposium on and 2011 Workshop on Scientific Use of Submarine Cables and Related Technologies (SSC), Underwater Technology (UT)* (2011), 1-7.

[10] P. King, A. Vardy, P. Vandrish, B. Anstey, Real-time side scan image generation and registration framework for AUV route following, *Autonomous Underwater Vehicles (AUV), 2012 IEEE/OES* (2012), 1-6.